

# Impulse Radio UWB Signal Detection Based on Compressed Sensing

Xing Zhu, Youming Li, Xiaoqing Liu, Ting Zou, Bin Chen

Institute of Communication Technology, Ningbo University, Ningbo, China

Email: liyouming@nbu.edu.cn

Received June, 2013

## ABSTRACT

The extremely high sampling rate is a challenge for ultra-wideband (UWB) communication. In this paper, we study the compressed sensing (CS) based impulse radio UWB (IR-UWB) signal detection and propose an IR-UWB signal detection algorithm based on compressive sampling matching pursuit (CoSaMP). The proposed algorithm relies on the fact that UWB received signal is sparse in the time domain. The new algorithm can significantly reduce the sampling rate required by the detection and provides a better performance in case of the low signal-to-noise ratio when comparing with the existing matching pursuit (MP) based detection algorithm. Simulation results demonstrate the effectiveness of the proposed algorithm.

**Keywords:** IR-UWB; Compressed Sensing; CoSaMP; MP; Signal Detection

## 1. Introduction

UWB is one of the key technologies in the short-range broadband wireless communication. With the characteristics of high data rates, low power, and low cost, UWB can be applied to many scenarios such as high-speed short-range wireless personal area networks (WPAN), ranging, positioning, monitoring, and wireless sensor networks (WSN) [1]. In some of these applications, UWB signal detection is a very important component. Hence there is a need to study the UWB signal detection to make it more practical.

However, when using the traditional algorithm for UWB signal detection, a very high sampling rate is required according to Shannon-Nyquist sampling theorem for the UWB signal's high bandwidth that is up to several gigahertz. This is difficult to implement with a practical analog-to-digital converter (ADC) [2]. The emerging theory of CS enables the reconstruction of sparse or compressible signals from a small set of random measurements. If adopted by the signal detection, the CS theory will make the sampling rate much lower than the Nyquist rate. The authors in [3,4] proved that it is effective to detect signal by processing the sampling values of compressed sensing directly. Reference [5] proposed a MP based signal detection algorithm. In [2], the authors proposed a CS based system for UWB echo signal detection at a sampling rate much lower than Nyquist rate. This study indicates that the low-dimensional random measurement method based on the CS theory can be used to sample UWB signal. A UWB signal detection

method based on MP algorithm was developed in [6]. Whereas in a circumstance with low signal-to-noise ratio (SNR), the performance of the MP based detection algorithm is not good. Thus, it leaves room for improvement. In [7], the authors demonstrated that CS theory is particularly suitable to IR-UWB signal detection, and a generalized likelihood ratio test (GLRT) detector was proposed. However, the GLRT UWB receiver needs the pilot symbol assisted modulation, leading to high system complexity. Furthermore, in order to reach a high performance, the number of mixer-integrators employed by the receiver is too large to be realized.

In this paper, we propose a CoSaMP [8] based IR-UWB signal detection method. Without other extra processes, the method is formed from extracting information directly from sampling values acquired by CS. The complexity of the proposed detection method is reduced dramatically when comparing with the GLRT detector. Moreover, computer simulation results are provided to verify the performance of the proposed method, which show that the performance of the new method is superior to that of the MP based detection algorithm, especially in low signal-to-noise ratio.

The remainder of the paper is organized as follows. In Section II, the background of CS is depicted. Section III provides the principle for generating IR-UWB signal. Section IV presents a CS based IR-UWB signal detection principle and proposes a CoSaMP based IR-UWB signal detection algorithm. Simulation results are provided in Section V. Finally, conclusions are drawn in Section VI.

## 2. Compressed Sensing Background

CS is a technology that can recover the high-dimensional signals from the low-dimensional and sub-Nyquist sampling data with the prior information that the signals are sparse or compressible [9]. The mathematical model of CS can be described as

$$\mathbf{y} = \mathbf{A}\mathbf{x} \quad (1)$$

where  $\mathbf{x} \in \mathbf{R}^{N \times 1}$  is a signal which can be sparsely represented in a basis matrix  $\boldsymbol{\varphi} = \{\varphi_1, \varphi_2, \dots, \varphi_N\} \in \mathbf{R}^{N \times N}$ , that is,  $\mathbf{x} = \boldsymbol{\varphi}\boldsymbol{\theta}$ , the vector  $\boldsymbol{\theta} = [\theta_1, \theta_2, \dots, \theta_N]^T \in \mathbf{R}^{N \times 1}$  consists of  $K$  ( $K \ll N$ ) nonzero elements (we often say that  $\boldsymbol{\theta}$  is  $K$ -sparse). The vector  $\mathbf{A} \in \mathbf{R}^{M \times N}$  ( $K < M \ll N$ ) is a random measurement matrix that is uncorrelated with  $\boldsymbol{\varphi}$ .  $\mathbf{y} \in \mathbf{R}^{M \times 1}$  denotes the  $M$  samples obtained by CS. Our purpose is to recover the sparse coefficient vector  $\boldsymbol{\theta}$  from the  $M$  samples, and then multiply it by the basis matrix  $\boldsymbol{\varphi}$ , thus recovering the original signal  $\mathbf{x}$ .

In order to figure out the sparse coefficient vector  $\boldsymbol{\theta}$ , we need to find the solution to the following  $l_0$  norm optimization problem [10]

$$\hat{\boldsymbol{\theta}} = \arg \min \|\boldsymbol{\theta}\|_0 \quad s.t. \quad \mathbf{y} = \mathbf{A}\boldsymbol{\varphi}\boldsymbol{\theta} \quad (2)$$

Unluckily, solving the optimization problem (2) is prohibitively complex for it is an NP-hard nonconvex optimization problem. A modified problem is to replace the  $l_0$  restrict with the  $l_1$  restrict

$$\hat{\boldsymbol{\theta}} = \arg \min \|\boldsymbol{\theta}\|_1 \quad s.t. \quad \mathbf{y} = \mathbf{A}\boldsymbol{\varphi}\boldsymbol{\theta} \quad (3)$$

This optimization problem transforms (2) into a convex optimization problem which can be easily solved by linear programming.

## 3. Impulse Radio UWB Theory

The US Federal Communications Commission (FCC) provided a definition that a signal can be classified as an UWB signal if its fractional bandwidth is greater than 0.2 or its bandwidth is 500MHz or more [1]. According to this definition, there are several ways to generate UWB signals, among which impulse radio is the most common method. In this paper, we focus on the impulse radio UWB (IR-UWB) signal.

IR-UWB communication is based on transmitting ultra-short (typically on the order of a nanosecond) duration pulses that are subsequently modulated by the binary information symbols. The two most popular modulation schemes are pulse amplitude modulation (PAM) and pulse position modulation (PPM).

Owing to different approaches are employed to generate the pulse train, the UWB systems can be divided into two main categories: time hopping UWB (TH-UWB) and direct sequence UWB (DS-UWB). To take a specific case, we will discuss the PAM-DS-UWB signal and its

detection in the following. A block diagram of the PAM-DS-UWB transmitter [1] is shown in **Figure 1**.

In **Figure 1**,  $\mathbf{b} = (\dots, b_0, b_1, \dots, b_k, b_{k+1}, \dots)$  is a binary sequence to be sent and generated at a rate of  $R_b = 1/T_b$  (bits/s). After passing through the repeat encoder, every bit of the sequence  $\mathbf{b}$  is repeated  $N_s$  times, therefore we get a new sequence

$$\mathbf{b}^* = (\dots, b_0, b_0, \dots, b_0, b_1, b_1, \dots, b_1, \dots, b_k, b_k, \dots, b_k, \dots)$$

where  $\mathbf{b}^*$  has a rate of  $R_{cb} = N_s/T_b = 1/T_s$  (bits/s). Then the second system of the block diagram converts  $\mathbf{b}^*$  into a sequence  $\mathbf{m} = (\dots, m_0, \dots, m_1, \dots, m_j, m_{j+1}, \dots)$  that contains two kinds of elements,  $+1$  and  $-1$ . The conversion equation of this is  $m_j = 2b_j^* - 1$  ( $-\infty < j < +\infty$ ). When the sequence  $\mathbf{m}$  enters the transmission encoder, a binary zero correlation duration (ZCD) code

$$\mathbf{a} = (\dots, a_0, a_1, \dots, a_j, a_{j+1}, \dots)$$

composed of  $\pm 1$ 's is applied to it [11] and the output of the transmission encoder is a new sequence  $\mathbf{m}^*$ , which can be expressed as

$$\begin{aligned} \mathbf{m}^* = & (\dots, m_0 a_0, m_0 a_1, \dots, m_0 a_j, \\ & \dots, m_1 a_0, m_1 a_1, \dots, m_1 a_j, \dots \\ & \dots, m_j a_0, m_j a_1, \dots, m_j a_j, \dots) \\ = & (\dots, m_0^*, m_1^*, \dots, m_j^*, \dots) \end{aligned} \quad (4)$$

The period of the ZCD code

$$\mathbf{a} = (\dots, a_0, a_1, \dots, a_j, a_{j+1}, \dots)$$

is  $N_p$ , we often assume that  $N_p = N_s$  (a more general hypothesis is that  $N_p$  is an integer multiple of  $N_s$ ). The rate of sequence  $\mathbf{m}^*$  is  $R_c = N_s/T_b = 1/T_s$  (bits/s). Next, the sequence  $\mathbf{m}^*$  goes into the PAM modulator, and a sequence of unit pulses (Dirac pulses  $\delta(t)$ ) located at times  $jT_s$  are generated by the PAM modulator [1,11]. The rate of the sequence of unit pulses is  $R_p = N_s/T_b = 1/T_s$  (pulses/s). At last, the output of the PAM modulator passes through the pulse shaper, whose impulse response is  $p(t)$ . The duration of  $p(t)$  is  $T_m$ , and  $T_m \ll T_s$ . Thus, we get the final output signal  $s(t)$ , which is given by

$$s(t) = \sum_{j=-\infty}^{+\infty} m_j^* p(t - jT_s) \quad (5)$$

where  $p(t)$  often has the following form

$$p(t) = (1 - 4\pi \frac{t^2}{\alpha^2}) e^{-\frac{2\pi t^2}{\alpha^2}} \quad (6)$$

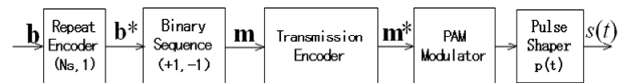


**Figure 1.** Block diagram of PAM-DS-UWB transmitter.

where  $\alpha^2 = 4\pi\sigma^2$  is the pulse shaper factor, and  $\sigma^2$  is the variance.

In practice, a PAM-DS-UWB transmitter's parameters set by the user are: the average transmit power  $P_0$ , the number of bits generated by the binary source  $n_0$ , the sampling frequency  $f_c$ ,  $N_p$ ,  $T_s$ ,  $N_s$ ,  $T_m$ , and  $\alpha^2$  [1].

**Figure 2** shows an example of the PAM-DS-UWB signal. From this figure, we can see that PAM-DS-UWB signal presents an intuitive sparse characteristic in the time domain. That is, the signal has only a few nonzero values. Thus, according to the Section II, the basis matrix of the PAM-DS-UWB signal can be an identity matrix.

Based on the above, we can apply the CS theory into the PAM-DS-UWB signal detection.

## 4. CS Based IR-UWB Signal Detection

### 4.1. The Signal Detection Model

We implement the detection by distinguishing between the following two hypotheses

$$\begin{aligned} H_0 : \mathbf{y} &= \mathbf{A}\mathbf{n} \\ H_1 : \mathbf{y} &= \mathbf{A}(\mathbf{x} + \mathbf{n}) \end{aligned} \quad (7)$$

where  $\mathbf{x} \in \mathbf{R}^{N \times 1}$  denotes the PAM-DS-UWB signal to be detected, and  $\mathbf{n} \sim N(0, \sigma^2 \mathbf{I}_N)$  is the independent and identically distributed additive white Gaussian noise.  $\mathbf{A} \in \mathbf{R}^{M \times N}$  ( $M \ll N$ ) is a known random measurement matrix, and  $\mathbf{y} \in \mathbf{R}^{M \times 1}$  is the sample obtained by the detector. Next, we let

$$\begin{aligned} P_d &= \Pr(H_1 \text{ chosen when } H_1 \text{ true}) \text{ and} \\ P_f &= \Pr(H_1 \text{ chosen when } H_0 \text{ true}) \end{aligned}$$

denote the probability of detection and the probability of false alarm respectively [3].

**Figure 3** illustrates the principle block diagram of the IR-UWB signal detection based on CS.

### 4.2. The Proposed IR-UWB Signal Detection Algorithm

In this section, we propose an IR-UWB signal detection algorithm based on CoSaMP [8]. The procedure of the algorithm is as follows:

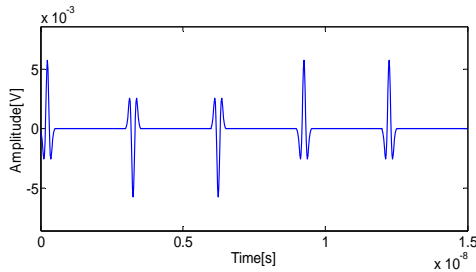


**Figure 2.** PAM-DS-UWB signal.

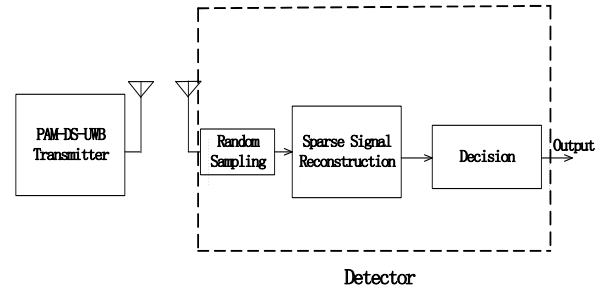


**Figure 3.** IR-UWB signal detection principle block diagram.

Let  $\Phi \in \mathbf{R}^{M \times N}$  denote the measurement matrix with restricted isometry constant  $\delta_{2s} \leq c$  ( $c$  is a constant),  $\mathbf{u}$  denote the noisy sample vector. Furthermore, the sparsity level (the number of the nonzero values) is  $s$ , and the  $s$ -sparse approximation of the target signal is  $\mathbf{a}$ .

a) Initialize the approximation  $\mathbf{a}_0 = 0$  and residual  $\mathbf{v} = \mathbf{u}$ . Initialize the iteration counter  $k = 1$ .

b) Find a proxy  $\mathbf{y} = \Phi^* \mathbf{v}$  for the current residual and locate the  $2s$  largest columns of the proxy

$$\Omega = \text{supp}(\mathbf{y}_{2s})$$

where  $\text{supp}(\mathbf{y}_{2s})$  means the index set of the  $2s$  largest columns of  $\mathbf{y}$ .

c) Merge the index set of the newly identified components with that of the largest components of the current approximation

$$T = \Omega \cup \text{supp}(\mathbf{a}_{k-1})$$

d) Solve a least squares problem to make an estimation of the signal

$$\mathbf{b}|_T = \Phi_T^\dagger \mathbf{u}; \quad \mathbf{b}|_{T^c} = 0$$

where  $\Phi_T^\dagger = (\Phi_T^* \Phi_T)^{-1} \Phi_T^*$ . For an arbitrary  $\mathbf{b} \in \mathbf{R}^{N \times 1}$ , assume that  $T$  is a subset of  $\{1, 2, \dots, N\}$ , we define

$$\mathbf{b}|_T = \begin{cases} b_i, & i \in T \\ 0, & \text{otherwise} \end{cases}$$

e) Reserve the  $s$  largest components in the approximation obtained by the step d) to produce a new approximation

$$\mathbf{a}_k = \mathbf{b}_s$$

f) Update the residual

$$\mathbf{v} = \mathbf{u} - \Phi \mathbf{a}_k$$

g)  $k = k + 1$ , if  $\|\mathbf{v}\|_2 \leq \varepsilon$ , where  $\varepsilon$  is a known constant, then go to step b); or else, go to step h).

h) If  $\|a\|_\infty > \lambda$ , where  $\lambda$  is a threshold value, then detect  $H_1$ ; otherwise, choose  $H_0$ .

## 5. Simulation Results

In this section, the performance of the proposed detection algorithm and the MP based detection algorithm are compared. First, we set the parameters of the PAM-DS-

UWB transmitter as follows:  $P_0 = -30$  (dBm),  $n_0 = 2$ ,  $f_c = 50e9$  (Hz),  $N_p = 10$  (s),  $T_s = 3e-9$  (s),  $N_s = 5$ ,  $T_m = 0.5e-9$  (s),  $\alpha^2 = 0.25e-9$ . Hence the length of the PAM-DS-UWB signal to be detected is

$$N = n_0 * N_s * f_c * T_s = 1500 \quad [12].$$

We set the sparsity level of the signal as  $s = 250$ . The signal is shown in **Figure 4**.

In simulation, we let the measurement matrix  $\mathbf{A} \in \mathbf{R}^{M \times N}$  be an independent and identically distributed Gaussian random matrix with zero-mean and unit variance. Further, the mean and variance of the additive white Gaussian noise are 0 and 1, respectively. For the proposed detection algorithm, we let constant  $\varepsilon = 10^{-5}$ . For the MP based detection algorithm [5], we set the number of iterations as 10. Suppose that the prior probabilities of the two hypotheses are equal, that is,  $P_r(H_0) = P_r(H_1) = 0.5$ . The probability of detection is the statistic result of 10000 trials. In order to demonstrate the effectiveness of the proposed algorithm, we have implemented the following three simulations.

**Figure 5** illustrates  $P_d$  as a function of  $M$  which is the number of measurements. We set the SNR as -2dB, and  $P_f = 0.01$ .  $M$  ranges [150, 750]. The threshold value  $\lambda$  and the threshold value of MP based detection algorithm are both chosen by Monte Carlo simulations [5]. The number of Monte Carlo simulations is 2000. If we use the traditional detection algorithm, the number of measurements should be  $N = n_0 * N_s * f_c * T_s = 1500$  according to the Shannon-Nyquist sampling theorem. As we can see from this figure, the proposed algorithm can acquire a very high probability of detection at about 20% of the sampling rate required by the Shannon-Nyquist theorem. What's more, in this condition, the proposed algorithm is superior to the MP based detection algorithm.

**Figure 6** shows  $P_d$  as a function of the SNR which ranges [-10, 5]. We consider  $M = 300$  and  $M = 500$  respectively. Let  $P_f = 0.01$ . The threshold values of the two algorithms under different SNRs are also acquired by the same means as in **Figure 5**. According to **Figure 6**, we can see that the performance of the proposed algorithm is better than that of the MP based detection algorithm when the SNR is less than -1 dB.

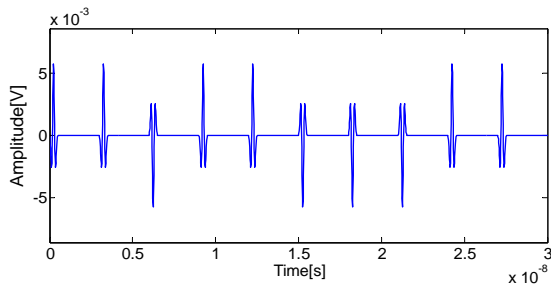


**Figure 4.** The PAM-DS-UWB signal of interest.

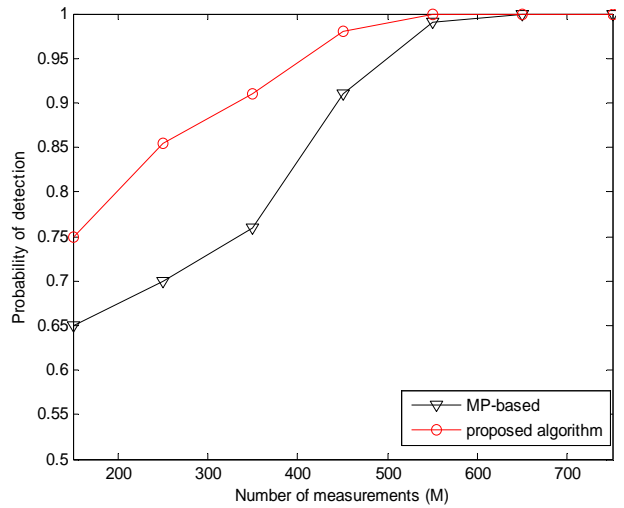


**Figure 5.** Probability of detection comparison of the proposed algorithm and the MP based detection algorithm under different number of measurements, SNR=-2 dB and  $P_f = 0.01$ .

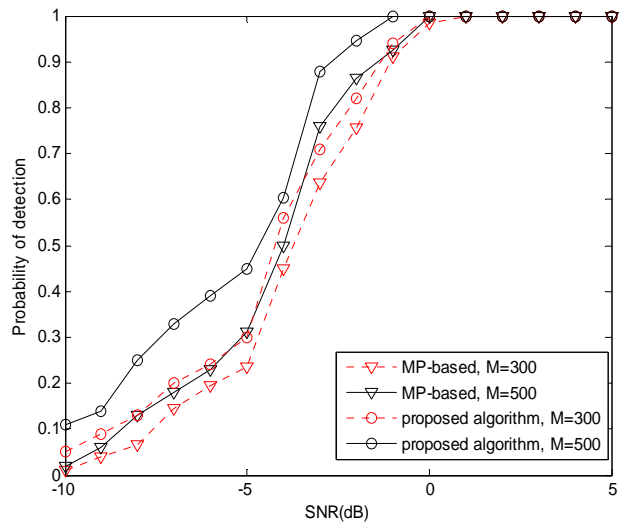


**Figure 6.** Probability of detection comparison of the proposed algorithm and the MP based detection algorithm under different SNRs,  $M = 300$  or  $M = 500$ ,  $P_f = 0.01$ .

**Figure 7** illustrates  $P_d$  as a function of  $P_f$  which ranges [0, 0.2]. Let  $M = 150$  and SNR= -2 dB. The threshold values of the two algorithms under different probabilities of false alarm are chosen by using the method in **Figure 5** and **Figure 6**. As we can see from **Figure 7**, the proposed algorithm is superior to the MP based detection algorithm in this situation.

According to **Figure 5**, **Figure 6** and **Figure 7**, we can speculate that the performance of the proposed IR-UWB signal detection algorithm is better than that of the MP based detection algorithm in case of the low SNR. Meanwhile, the proposed algorithm needs a much lower sampling rate than the Nyquist rate.

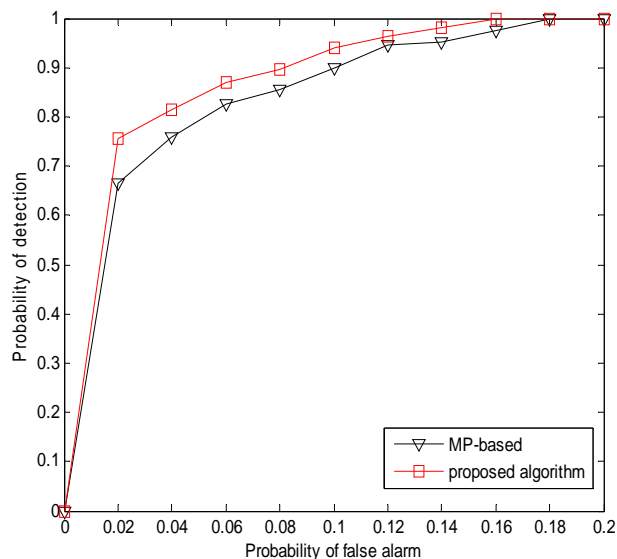


**Figure 7. Probability of detection comparison of the proposed algorithm and the MP based detection algorithm under different probabilities of false alarm,  $M = 150$ ,  $SNR = -2$  dB.**

## 6. Conclusions

In this paper, we present a CS based IR-UWB signal detection model and an IR-UWB signal detection algorithm based on CoSaMP. Compared with the GLRT based model, the proposed model is easier to realize. The new detection algorithm solves the detection problem by directly processing the sampling values obtained by CS. It is proved that the proposed algorithm can detect the IR-UWB signal at a sampling rate that is much lower than the Nyquist rate. Numeric simulations show that the new algorithm yields performance gains over the MP based detection algorithm in case of the low SNR.

## 7. Acknowledgements

This work was supported in part by the National Science Foundation of China (61071119), Scientific and Technological Innovations Teams of Zhejiang Province (2010R50009), Ningbo Natural Science Foundation (2012A610017), and Innovation Team of Ningbo (No. 2011B81002).

## REFERENCES

- [1] M. D. Benedetto and G. Giancola, "Understanding Ultra Wide Band Radio Fundamentals," Upper Saddle River, NJ: Prentice Hall, 2004.
- [2] G. Shi, J. Lin, X. Chen, *et al.*, "UWB Echo Signal Detection with Ultra-low Rate Sampling based on Compressed Sensing," *IEEE Transactions on Circuits and Systems*, Vol. 55, No. 4, 2008, pp. 379-383. [doi:10.1109/TCSII.2008.918988](https://doi.org/10.1109/TCSII.2008.918988)
- [3] M. A. Davenport, M. B. Wakin and R. G. Baraniuk, "Detection and Estimation with Compressive Measurements," Elect. Comput. Eng. Dept., Rice University, Houston, Tx, 2006, Tech. Rep. TREE0610.
- [4] J. Haupt and R. Nowak, "Compressive Sampling for Signal Detection," in *Proc. IEEE Int. Conf. Acoust., Speech, Signal Process. (ICASSP)*, Honolulu, HI, April 2007, pp. 1509-1512.
- [5] M. F. Duarte, M. A. Davenport, M. B. Wakin and R. G. Baraniuk, "Sparse Signal Detection from Incoherent Projections," in *Proc. IEEE Int. Conf. Acoust., Speech, Signal Process. (ICASSP)*, Toulouse, France, May 2006, pp. 305-308.
- [6] J. L. Paredes, G. R. Arce and Z. Wang, "Ultra-wideband Compressed Sensing: Channel Estimation," *IEEE J. Select. Topics Signal Process.*, Vol. 1, No. 3, pp. 383-395, 2007.
- [7] Z. Wang, G. R. Arce, J. L. Paredes and B. M. Sadler, "Compressed Detection for Ultra-wideband Impulse Radio," in *Proc. of 8th IEEE Int. Workshop SPAWC*, June 2007, pp. 1-5.
- [8] D. Needell and J. A. Tropp, "CoSaMP: Iterative Signal Recovery from Incomplete and Inaccurate Samples," *Applications and Computational Harmonic Analysis*, Vol. 26, No. 3, 2009, pp. 301-321. [doi:10.1016/j.acha.2008.07.002](https://doi.org/10.1016/j.acha.2008.07.002)
- [9] L. Jiao, S. Yang, F. Liu, and B. Hou, "Development and prospect of compressive sensing," *Acta Electronica Sinica*, Vol. 39, No. 7, 2011, pp.1651-1662.
- [10] P. Zhang, Z. Hu, R. C. Qiu and B. M. Sadler, "A Compressed Sensing Based Ultra-wideband Communication System," in *Proc. IEEE Int. Conf. Communications (ICC)*, Dresden, Germany, June 2009, pp. 1-5.
- [11] E. C. Kim, S. Park, J. S. Cha and J. Y. Kim, "Improved Performance of UWB System for Wireless Body Area Networks," *IEEE Transactions on Consumer Electronics*, Vol. 56, No. 3, 2010, pp. 1373-1379. [doi:10.1109/TCE.2010.5606272](https://doi.org/10.1109/TCE.2010.5606272)
- [12] L. Shi, "Applied Research on Compressed Sensing for Ultra Wideband Channel Estimation," Ph.D. Thesis, Beijing University of Posts and Telecommunications, 2011.